hep-ph/9902266 8 Feb 1999

Parameterisation of $[\sigma_{1/2} - \sigma_{3/2}]$ for $Q^2 \geq 0$ and non-resonance contribution to the GDH sum rule

N. Bianchi† and E. Thomas

INFN-Laboratori Nazionali di Frascati

CP 13, I-00044 Frascati, Italy

February 27, 1999

Abstract

A description of the virtual photon absorption cross section difference $\left[\sigma_{1/2} - \sigma_{3/2}\right]$ for the proton and neutron is obtained with a parameterisation based on a Regge type approach. The parametrisation is obtained from global fits to the cross section data derived from the spin asymmetries measured in deep inelastic scattering of longitudinally polarised leptons from polarised ^{1}H, ^{3}He and ^{2}H targets in the range 0.3 GeV^2 $< Q^2 <$ 70 GeV^2 and 4 GeV^2 $< W^2 <$ 300 GeV^2. The fits give a reliable description of the data and provide predictions for the photo-production through a smooth Q^2-transition. The contribution above the resonance region to the Gerasimov-Drell-Hearn sum rule for real and virtual photons has been evaluated. For the real photons this contribution accounts for a large fraction of the discrepancy between the sum rule expectations and the single pion photo-production analysis estimates.

PACS numbers : 13.60.Hb; 13.88.+e; 25.20.Dc; 25.30.Fj
Keywords : Deep Inelastic Scattering, Sum Rules, Asymmetries, Photo-absorption.

† Corresponding author: Nicola.Bianchi@lnf.infn.it

1 Introduction

The study of deep-inelastic-scattering (DIS) of polarised leptons off polarised nucleons provides information on the spin composition of the nucleon. The experimental cross section asymmetry is generally written in terms of the target nucleon polarised structure functions which have been successfully interpreted in terms of parton spin distributions. In this paper we analysed the available experimental data in terms of the virtual photon-nucleon polarised cross sections which describe the multi-hadron polarised electroproduction. This approach is complementary to the usual description of the interaction of the probing virtual photon with the constituent partons. It allows to extend the description of the process to the real photon case in which the interactions can be unambiguously interpreted in terms of cross sections only. The relevant quantity of our interest is the difference of the cross sections $\Delta\sigma = \left[\sigma_{1/2} - \sigma_{3/2}\right]$ in which $\sigma_{1/2}$ and $\sigma_{3/2}$ are the photon-nucleon absorption cross section of total helicity 1/2 and 3/2, respectively.

A fundamental sum rule for this quantity has been derived by Gerasimov, Drell and Hearn[1] (GDH). It relates the anomalous contribution κ to the magnetic moment of the nucleon ($\kappa_{\rm p}$=1.79, $\kappa_{\rm n}$=−1.91) with the total absorption cross sections for circularly polarised real photons on polarised nucleons. It is given by:

$$I = \int_{\nu_0}^{\infty} \Delta\sigma(\nu)\frac{d\nu}{\nu} = -\frac{2\pi^2\alpha}{m^2}\kappa^2, \tag{1}$$

where ν is the photon energy, ν_0 is the pion photoproduction threshold and m is the nucleon mass. The theoretical predictions for the integral are −204 μb, −233 μb and +29 μb for the proton, neutron and proton-neutron difference (p-n), respectively. Experimentally this sum rule has never been tested directly because of the lack of suitable polarised targets and real photon beams. Several experiments are planned at different facilities to measure the spin-dependent photo-production cross section in the nucleon resonance region and up to about 3 GeV[2]. Multipole analysis of single pion photo-production amplitudes and estimates of the double pion contribution from the nucleon resonance decays provided an indication of the low energy contribution to the sum rule, which is expected to be the dominant one. These estimates were qualitatively consistent among each others providing results ranging between −289 and −257 μb, −189 and −169 μb, −130 and −68 μb for the proton, neutron and proton-neutron difference respectively[3-7]. All these findings strongly disagree with the GDH expectations and suggested a possible violation of the sum rule. In particular the multipole analysis of the isovector channel (i.e. the proton-neutron difference) provides an opposite sign of the sum rule expectation.

The integral defined in Eq. 1 can be generalised to the absorption of virtual photons with energy ν and squared four-momentum $-Q^2$:

$$I(Q^2) = \int_{\nu_0}^{\infty} \Delta\sigma(\nu, Q^2)\frac{d\nu}{\nu}. \tag{2}$$

In the limit $Q^2/\nu^2 \ll 1$ the above integral is connected to the first momentum Γ_1 of the nucleon spin structure function $g_1(x)$ over the Bjorken variable x [8]:

$$I(Q^2) \approx I_1(Q^2) = \frac{16\pi^2\alpha}{Q^2}\Gamma_1 = \frac{16\pi^2\alpha}{Q^2}\int_0^1 g_1(x)dx. \tag{3}$$

It is worth noting that in the transition region, from Q^2=0 to DIS regime, $I_1(Q^2)$ is only an approximation of $I(Q^2)$ [9]; therefore a determination of $[\sigma_{1/2} - \sigma_{3/2}]$ is needed for a precise evaluation of the Q^2 dependence of the generalised GDH integral, defined by Eq. 2. Several measurements are planned at TJNAF to measure the resonance region contribution to the generalised GDH integral $I(Q^2)$[10].

In this work we analysed the available polarised deep inelastic scattering data to evaluate the contribution above the resonance region to the generalised GDH integral $I(Q^2)$ and to provide an estimate for the real photon limit. A Regge inspired parameterisation was used.

2 Regge phenomenology

The Regge theory provided a good description of the high-energy behaviour of the cross sections for a large number of processes[11]. In this framework the cross section behaviours are given by $\sigma \sim s^{\alpha^0-1}$

where s is the centre of mass square energy and α^0 is the intercept of the leading Regge trajectory for the given process. The intercept $\alpha^0 = J - \alpha' m_t^2$ is determined by the spin J and mass m_t of the exchanged particle and by the trajectory slope $\alpha' \simeq 0.8\text{-}0.9$ GeV^{-2}. In the case of the absorption of circularly polarised photons on polarised nucleon it is useful to consider the isovector and the isoscalar terms of the interaction[12].

The isovector contribution to $\Delta\sigma$ is described by the $a_1(1260)$ meson trajectory : $\Delta\sigma_V \sim s^{\alpha^0_{a1}-1}$. The axial vector meson a_1 is still now an elusive prey in most of experiments due to its large width and the presence of strong background. Experiments of the last twenty years provided contradictory measurements of the a_1 meson mass and width over the wide ranges 1.05-1.28 GeV and 0.24-0.61 GeV, respectively[13]. The expected value of the a_1 meson intercept is about -0.3, but due to the uncertainties in the knowledge of the mass and of the trajectory slope, a possible range between 0 and -0.5 is generally considered.

The isoscalar contribution to $\Delta\sigma$ is described by the $f_1(1285)$ meson trajectory $\Delta\sigma_I \sim s^{\alpha^0_{f1}-1}$. Being the f_1 meson mass well known, its intercept is expected to be about -0.4 ± 0.1. In addition it has been shown that the exchange of two non-perturbative gluons can provide an isoscalar contribution $\Delta\sigma_I \sim (1/s) ln(s/\mu^2)$ where the mass parameter μ has the typical hadronic scale $\mu \sim 1$ GeV[14].

In this work we consider the above described contributions for the case of photo-absorption of circularly polarised virtual photon on polarised nucleon where the centre of mass square energy is given by $W^2 = m^2 + 2m\nu - Q^2$.

3 Data analysis and fitting procedure

We have analysed the data from deep inelastic scattering of longitudinally polarised leptons off polarised ^{1}H, ^{2}H and ^{3}He targets which provided measurements of the photo-absorption asymmetry A_1 for the proton, deuteron and neutron respectively. The measurements were performed by six experiments at CERN (EMC[15], SMC[16]), SLAC (E142[17], E143[18], E154[19]) and DESY (HERMES[20]). For each experiment we considered the data set with the most detailed Q^2 and x binnings. Therefore we did not include in the fit the Q^2-averaged data which are generally used for the determination of the polarised structure function $g_1(x)$. A total of 511 independent data points was included in the analysis: specifically 238 proton data, 81 neutron data and 192 deuteron data. The kinematic range covered by the data is $0.3\ \text{GeV}^2 < Q^2 < 70\ \text{GeV}^2$ and $4\ \text{GeV}^2 < W^2 < 300\ \text{GeV}^2$ for the proton and deuteron, and $1\ \text{GeV}^2 < Q^2 < 15\ \text{GeV}^2$ and $4\ \text{GeV}^2 < W^2 < 70\ \text{GeV}^2$ for the neutron.

The cross section difference $\Delta\sigma$ was derived from the measured virtual photo-absorption asymmetry A_1 and from the unpolarised structure function F_1:

$$\Delta\sigma = 2A_1\sigma_T = \frac{8\pi^2\alpha}{m}\,\frac{A_1F_1}{K}, \tag{4}$$

where σ_T is the total transverse cross section and $K = \sqrt{\nu^2 + Q^2}$ is the virtual photon flux factor. The structure function $F_1 = F_2(1+\gamma^2)/(2x(1+R))$ was calculated from published parameterisations of the unpolarised structure functions F_2 [21] for the proton, neutron and deuteron and of $R = \sigma_L/\sigma_T$, the ratio of the absorption cross sections [22] for longitudinally and transversely polarised virtual photons. The structure function R was assumed to be independent of the target ($R^p = R^n = R^d$).

The $\Delta\sigma$ experimental data were reproduced by a global 3-D fit over the Q^2 and W^2 variables and the isospin dimension T:

$$\Delta\sigma = \Delta\sigma(T, W^2, Q^2) = \left[2aW^{2(\alpha^0_{a1}-1)}T + fW^{2(\alpha^0_{f1}-1)} + g\frac{lnW^2}{W^2}\right]F, \tag{5}$$

where F is the threshold factor

$$F = \left[\frac{W^2 - W_\pi^2}{W^2 - W_\pi^2 + Q^2 + m_r^2}\right]^p, \tag{6}$$

where $W_\pi = 1.12$ GeV is the single pion electro-production threshold and $m_r = 1.26$ GeV is a common mass scale of the exchanged particles which is close to the a_1 and f_1 meson masses and to the two gluon exchange hadronic scale. The exponent p is given by

$$p = 1.5\left(1 + \frac{Q^2}{Q^2 + M^2}\right), \tag{7}$$

being M a free parameter of the fit. This threshold factor is similar to the ones used in the description of unpolarised cross section σ_T accounting for the behaviour of a cross section corresponding to a virtual particle with $W^2 > Q^2$[23-26]. F increases from 0 at the pion electro-production threshold to ≈ 1 at high W^2, when $W^2 \gg Q^2$.

Because Regge theory gives no indication about the relative weight and Q^2-dependence of the various contributions, the three coefficients in eq. 5 were parametrised with a simple and smooth Q^2-dependence, with two free parameters each :

$$a, f, g = p_1^{a,f,g} + p_2^{a,f,g} t, \tag{8}$$

where

$$t = log\frac{log\frac{Q^2+Q_0^2}{\Lambda^2}}{log\frac{Q_0^2}{\Lambda^2}}. \tag{9}$$

Here Λ and Q_0^2 are the QCD cutoff and scale parameters, respectively. We used $\Lambda = 0.255$ GeV and $Q_0^2 = 0.278$ GeV^2 in agreement with the ALLM parameterisation for the unpolarised total transverse cross section σ_T[24].

The cross section difference for the proton and neutron were defined by eq. 5 with T=+1/2 and T=−1/2, respectively. The cross section difference for the deuteron was defined $\Delta\sigma^d = [\Delta\sigma^p + \Delta\sigma^n]\,(1 - 1.5\omega_D)$ where $\omega_D = 0.05$ is the D-wave probability in the deuteron[27].

4 Results

In the following we describe three different models we used to reproduce the $\Delta\sigma$ data. The results of the three models are presented in Table 1.

Model I

We fitted proton, neutron and deuteron data using the parameterisation described in the previous chapter and with 9 free parameters ($\alpha_{a1}^0, \alpha_{f1}^0, p_1^a, p_2^a, p_1^f, p_2^f, p_1^g, p_2^g, M^2$). The fit reproduced the data with reduced $\chi^2/ndf = 1.14$. The intercept of the f_1-meson trajectory was found within the expected range. On the contrary, the intercept of the a_1-meson trajectory was not consistent with the standard Regge theory. This finding may imply that the a_1-meson trajectory is strongly not linear or not parallel to the other meson trajectories (like the a_2-meson or the ρ-meson ones).

Model II

To cure the problem of non-linearity or non-parallelism of the previous model we introduced in the fit a smooth Q^2-dependence of a_1-meson intercept assuming it equal to 0 for Q^2=0 and varying linearly with t. With this assumption, the errors of the parameters of the coefficients and the χ^2/ndf were decreased. The intercept of the f_1-meson trajectory was found in excellent agreement with the expectation. The intercept of the a_1-meson trajectory changed of 0.25 in the Q^2 range 0-10 GeV^2. This behaviour is similar to the Q^2-evolution of the reggeon and the pomeron intercepts found in the description of the unpolarised σ_T data[24].

Model III

In this parameterisation, we considered an additional reggeon trajectory $2rW^{2(\alpha_r^0-1)}T$ for the isovector part of the interaction, with no Q^2-dependence of the intercepts. The result of this Model are only slightly worse respect to the ones of Model II. The intercept of the f_1-meson trajectory is within the expectation range. The intercept of the a_1-meson trajectory was found in excellent agreement with the expectation. The intercept α_r^0 of the additional reggeon trajectory was found close to the a_2-meson intercept ≈ 0.5.

All the three Models provide a rather good description of the present data. The new and precise data for proton and deuteron that will be provided by the HERMES and E155[28] collaborations will allow to better discriminate between the above described approaches. In the following, we show the results for the Model II which provided the best χ^2/ndf and which has the simplest phenomenological interpretation for the isovector component. The comparison between the results of Model II and the experimental data as

function of the three variables (T, W^2 and Q^2) is shown in fig. 1. For this purpose the data are presented grouped in Q^2-bins.

In fig. 1 are also shown the results of Model II for Q^2=0. The expectations for real photons are: $\Delta\sigma^p$ is positive up to $\nu \sim 150$ GeV, ranging between 0 and $\sim 23\mu$b; $\Delta\sigma^n$ is negative and ranges between ~ -14 and 0μb; $\Delta\sigma^d$ ranges between $+12$ and -4μb being positive below $\nu \sim 3.5$ GeV.

In fig. 2 the point to point difference between the fit of Model II and the experimental data is provided. The difference has been normalised by the statistical error of each data point. As it is seen the fit well reproduces all the data over the two orders of magnitude variation of the Q^2 and W^2 variables. The uniform distribution of this difference evidences the good quality of the fit and ensures a reliable extrapolation to $Q^2 = 0$.

A further comparison between Model II and experimental data is provided in fig. 3 where the expectations for the polarised structure functions $g_1(x)$ are shown. These were evaluated at $Q^2 = 3$ GeV^2 using eqs. 4 and 5 for model II under the approximation that $g_1(x, Q^2) \approx A_1(x)F_1(x, Q^2)$. The curves are compared with $g_1(x)$ Q^2-averaged data evolved at the same Q^2 and with a NLO-QCD fit based on polarised parton density distributions[29]. Our Model and the QCD model are in good agreement at least for $x \geq 0.03$ and both well reproduce the experimental data. At low-x, where they are different, the present experimental uncertainties are too large to provide strong constraints for both models. Measurements of the spin structure functions at very low-x using the HERA polarised collider[30] will shed light on this subject.

Also shown in fig. 3 are the a_1-meson, f_1-meson and two-gluons exchange individual contributions. In this framework, the stronger experimental variation of g_1^n at low-x respect to g_1^p is simply explained by the similar low-x behaviors of the isovector and the isoscalar components in the neutron. The change of sign of g_1^d is at $x \approx 0.015$ and is due to the different x-dependence of the two isoscalar components, being the f_1-meson positive contribution dominating at large-x, while the two-gluons negative one at low-x.

5 Contribution to the GDH integral

The Q^2-dependence of the high energy contribution ($W \geq 2$ GeV) $I_{he}(Q^2)$ to the generalised GDH integral $I(Q^2)$ can be evaluated from eq. 2 with a lower integration limit $\nu_0 = (4 - m^2 + Q^2)/2m$ GeV. In fig. 4 are shown the predictions for $I_{he}(Q^2)$ of Model II for the proton-neutron, proton, deuteron and neutron. Our result for the proton well reproduce the recent HERMES measurements [20] performed at fixed values of Q^2 and in which their Regge extrapolation for $\nu > 23.5$ GeV is taken into account. Also the E143 measurements[18] of the high energy contribution $I_{1he}(Q^2)$ to the integral $I_1(Q^2)$ for the proton and the deuteron are in reasonable agreement with our curves for $I_{he}(Q^2)$.

In fig. 4 are also shown our results of the total integral $I(Q^2) = I_{he}(Q^2) + I_{le}(Q^2)$ which includes the low energy contributions $I_{le}(Q^2)$ in the nucleon resonance region ($W < 2$ GeV). As it is seen the high energy contribution is the dominant one at high Q^2. At high Q^2, where the nucleon resonance excitation contribution is negligible and the approximation of eq. 3 is valid, our results well agree with the integrals I_1 measured by E143 at $Q^2 = 5$ GeV^2 [18] and by SMC at $Q^2 = 10$ GeV^2 [16].

The real photon limit $I_{he}(0)$ of the high-energy contribution to the GDH integral for the three Models and for the proton, neutron and proton-neutron difference are listed in Table 1. The three Model predictions are consistent among each other within $\sim 10\%$. Our predictions for the proton and deuteron are in agreement with the predictions $I_{he}^p = 25 \pm 10$ μb and $I_{he}^d \sim 0$ μb from ref.[31] in which a Regge-inspired approach was also used. In Table 1 the evaluations of the low-energy parts $I_{le}(0)$ are also presented. The latter results are more model dependent respect to the high-energy contributions and are strongly affected by the choice of the threshold factor F. Moreover $I_{le}(0)$ is less constrained by the experimental data and therefore provides only an approximate estimate of the multi-hadron and non-resonant photo-production contribution at low energy.

In Table 2 the $I_{he}(0)$ and $I_{le}(0)$ contributions, averaged over the three models, are reported. The quoted errors for the integrals were derived considering both the contribution of the free parameter errors and the contribution of the fit parameterisation. The latter, which is the dominant one for the real photon extrapolation, has been evaluated from the slightly different predictions of the three models, from varying the fixed parameters of the fit (Q_0^2, Λ^2, m_r^2) within a factor two around the chosen values and from a Q^2-independent choice of the power expression of the threshold function F.

In Table 2 we also reported the contributions from the most recent analysis of single-pion photo-production in both resonant and non-resonant channels [7] and from the decay of the nucleon resonances

in two-pions [3]. As it is seen the discrepancies between the sum of these two latter contributions and the GDH sum rule expectation is reduced by a factor ≥ 2 if we add our results for the high-energy contributions. Moreover the above discrepancies are almost canceled if we also include our estimates for the low-energy region.

Therefore the evaluation of multi-hadron photoproduction processes accounts for a relevant fraction of the GDH expectations for the proton and the neutron. In addition it represents the largest contribution for the isovector sum rule, in which the resonance contribution is mostly canceled. These phenomenological predictions will be soon tested by ongoing and upcoming experiments with real [2] and virtual photons of low Q^2 [10].

6 Conclusions

We have studied the deep inelastic scattering of longitudinally polarised leptons off polarised targets in terms of polarised cross sections. The cross sections have been fitted by three different parameterisations in which the isovector and the isoscalar contributions from Regge inspired models have been considered.

With these parameterisations we were able to well describe, over the whole kinematic range of Q^2 and W^2, the experimental polarised cross sections $\sigma_{1/2} - \sigma_{3/2}$ and structure functions g_1 for the proton, neutron and deuteron and the relevant integrals. We were able to evaluate the Q^2-evolution of the high energy contribution ($W \geq 2$ GeV) to the generalised GDH integral and to provide an accurate estimate for this contribution in the real photon limit. The latter contribution was found to be about one half of the present discrepancy between previous multipole analysis and the GDH sum rule expectations. Moreover we also provided a rough estimate of the low energy ($W < 2$ GeV) multi-hadron and non-resonance contribution to the GDH integral.

At present, while waiting for direct and experimental verifications, from the informations coming from unpolarised single-pion photo-production data at low energy and from inclusive polarised electro-production data at high energy, it seems reasonable to conclude that no room is left for a large violation of the GDH sum rule.

7 Acknowledgements

We would like to thank S.D. Bass for many suggestions and for reading the paper and G. Pancheri and K. Oganesyan for useful discussions. This work was partially supported by the TMR contribution (contract FMRX-CT96-0008) from the European Community.

References

[1] S.B. Gerasimov, Sov. J. Nucl. Phys. **2** (1966) 430; S.D. Drell and A.C. Hearn, Phys. Rev. Lett. **16** (1966) 908.

[2] N. Bianchi, Proc. Workshop on Electron Nucleus Scattering, O. Benhar and A. Fabrocini editors, Elba, July 1-5, 1996, p.363 and references therein.

[3] I. Karliner, Phys. Rev. **D 7** (1973) 2717.

[4] R.L. Workman and R.A. Arndt, Phys. Rev. **D 45** (1992) 1789.

[5] A.M. Sandorfi, C.S. Whisnant and M. Khandaker, Phys. Rev. **D 50** (1994) R6681.

[6] R.A. Arndt, I.I. Strakovsky and R. Workman, Phys. Rev. **C 53** (1996) 430.

[7] D. Drechsel and G.Krein, Phys. Rev. **D 58** (1998) 116009.

[8] M. Anselmino, B.L. Ioffe and E. Leader, Sov. J. Nucl. Phys. **49** (1989) 136.

[9] P. Slavich, Diploma Thesis, Università di Ferrara (1997), unpublished; R. Pantförder, PhD Thesis, Universität Bonn (1998), BONN-IR-98-06.

[10] V.D. Burkert *et al.*, CEBAF PR-91-23 (1991); S. Kuhn *et al.*, CEBAF PR-93-09 (1993); Z.E. Meziani *et al.*, CEBAF PR-94-10 (1994); J.P. Chen *et al.*, TJNAF PR-97-110 (1997).

[11] A. Donnachie and P.V. Landshoff, Phys. Lett. **B 296** (1992) 227.

[12] R.L. Heimann, Nucl. Phys. **B 64** (1973) 429.

[13] Particle Data Group, Phys. Rev. **D 54** (1996) 1.

[14] S.D. Bass and P.V. Landshoff, Phys. Lett. **B 336** (1994) 537.

[15] EMC Collaboration, J. Ashman *et al.*, Nucl. Phys. **B 328** (1989) 1.

[16] SMC Collaboration, B. Adeva *et al.*, Phys. Rev. **D 58** (1998) 112001.

[17] E142 Collaboration, P.L. Anthony *et al.*, Phys. Rev. **D 54** (1997) 6620.

[18] E143 Collaboration, K. Abe *et al.*, Phys. Rev. **D 58** (1998) 112003.

[19] E154 Collaboration, K. Abe *et al.*, Phys. Rev. Lett. **79** (1997) 26.

[20] HERMES Collaboration, K. Ackerstaff *et al.*, Phys. Lett. **B 444** (1998) 531; K. Ackerstaff *et al.*, Phys. Lett. **B 404** (1997) 383; A. Airapetian *et al.*, Phys. Lett. **B 442** (1998) 484.

[21] NMC Collaboration, M. Arneodo *et al.*, Phys. Lett. **B 364** (1995) 107.

[22] L.W. Whitlow *et al.*, Phys. Lett. **B 250** (1990) 193.

[23] A. Levy and U. Maor, Phys. Lett. **B 182** (1986) 108.

[24] H. Abramowicz, E.M. Levin, A. Levy and U. Maor, Phys. Lett. **B 269** (1991) 465.

[25] A. Capella, A. Kaidalov, C. Merino and J. Tran Thanh Van, Phys. Lett. **B 337** (1994) 358.

[26] P. Desgrolard, L. Jenkovszky and F. Paccanoni, hep-ex 9803286, to be published in Eur. Phys. J. **C**.

[27] R. Machleidt *et al.*, Phys. Rep. **149** (1987) 1.

[28] E155 Collaboration, C. Young, Proc. of the Workshop Deep Inelastic Scattering off Polarized Targets, J. Blümlein *et al.* editors, DESY 97-200 (1997) p.12.

[29] M. Gluck, E. Reya, M. Stratmann and W. Vogelsang, Phys. Rev. **D 53** (1996) 4775.

[30] A. De Roeck *et al.*, Eur. Phys. J. **C 6** (1999) 121.

[31] S.D. Bass and M.M. Brisudova, hep-ph 9711423, to be published in Eur. Phys. J. **C**.

Table 1: Parameter values and contributions to the GDH integral provided by the fit of the data with the different models. The error estimates have been obtained from a MINOS analysis of the MINUIT program.

	Model I	Model II	Model III
p_1^a [μb]	110±5	135±5	32 ±34
p_2^a [μb]	-41±4	-75±3	135 ±48
p_1^f [μb]	80±28	110±23	120±14
p_2^f [μb]	165±47	84±31	62±14
p_1^g [μb]	-21±2	-26±3	-32±2
p_2^g [μb]	20±2	23±2	24±2
p_1^r [μb]	-	-	41±2
p_2^r [μb]	-	-	-20±1
M^2 [GeV^2]	3.7±0.7	4.8±0.8	2.9±0.5
$\alpha^0_{a_1}$	0.16±0.02	$(0.20 \pm 0.02) \cdot t$	-0.27±0.03
$\alpha^0_{f_1}$	-0.49±0.10	-0.37±0.09	-0.51±0.15
α^0_r	-	-	0.43±0.02
χ^2/ndf	1.14	1.11	1.12
$I^p_{he}(0)$ [μb]	+28	+24	+27
$I^n_{he}(0)$ [μb]	−40	−32	−34
$I^d_{he}(0)$ [μb]	−10	−7	−6
$I^{p-n}_{he}(0)$ [μb]	+68	+55	+61
$I^p_{le}(0)$ [μb]	+27	+32	+25
$I^n_{le}(0)$ [μb]	−16	−14	−3
$I^d_{le}(0)$ [μb]	+10	+17	+20
$I^{p-n}_{le}(0)$ [μb]	+43	+45	+28

Table 2: Evaluation of the GDH integral I_{TOT} for the proton, neutron and proton-neutron difference and comparison with the relevant GDH sum rule expectations. I_{TOT} is computed by the sum of the predicted contributions for single-pion photo-production[7], double-pion photo-production from the decay of the nucleon resonances N^*[3], and for the high-energy ($W \geq 2$ GeV) and low-energy ($W < 2$ GeV) multi-hadron photo-production (this work).

	I_p [μb]	I_n [μb]	I_{p-n} [μb]
$I_{N\pi}$[7]	−196	−145	−51
$I_{N^*\to N\pi\pi}$[3]	−65	−35	−30
$I_{he}(0)$ this work	$+26 \pm 7$	-35 ± 11	$+61 \pm 12$
$I_{le}(0)$ this work	$+28 \pm 19$	-11 ± 14	$+39 \pm 29$
I_{TOT}	-207 ± 23	-226 ± 22	$+19 \pm 37$
GDH sum rule	−204	−233	+29

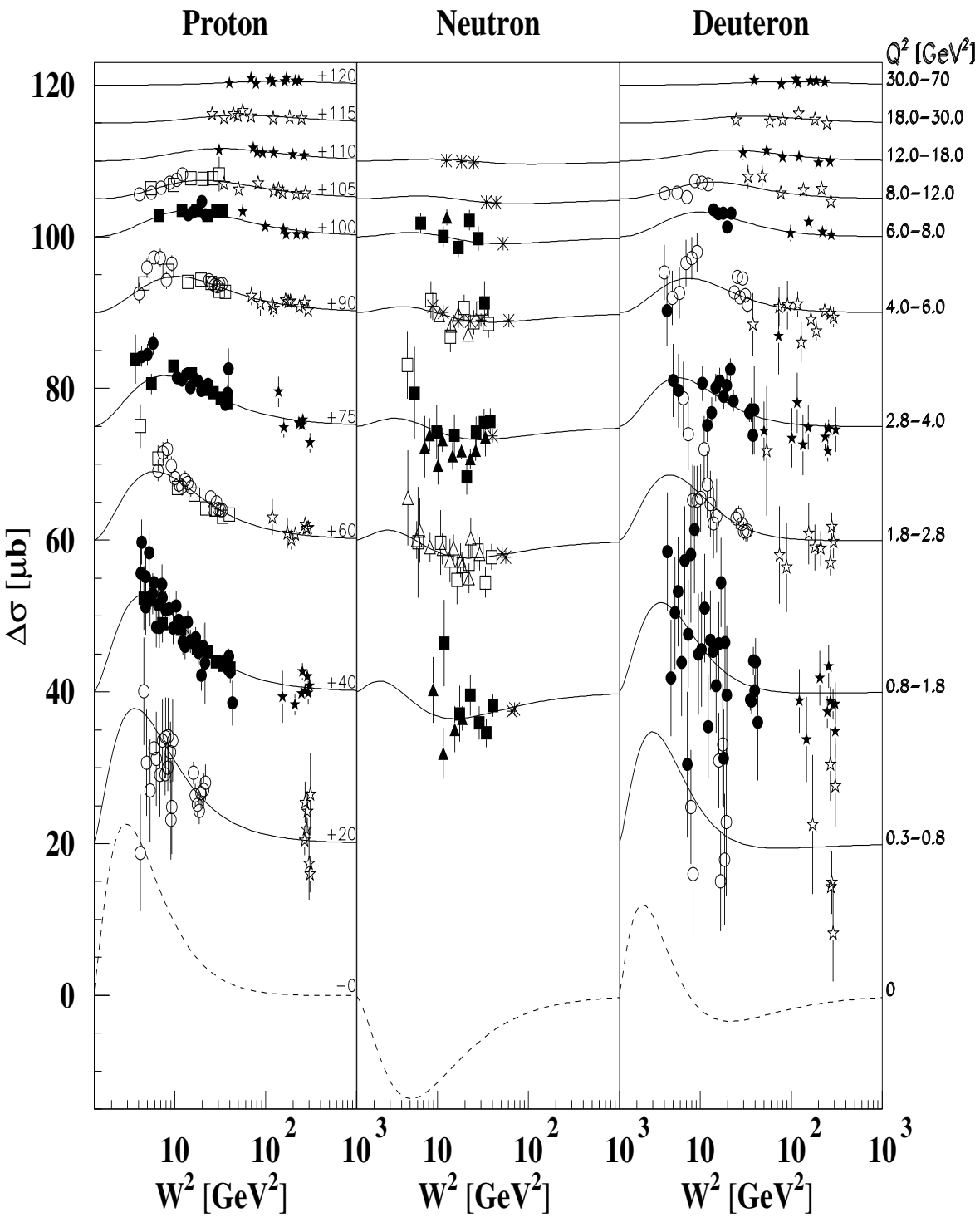

Figure 1: Cross section differences as a function of W^2 for different Q^2-bins (on the right scale). Data are from Refs. [15, 16] (stars), [17] (triangles), [18] (circles), [19] (asterisks), and [20] (squares). For a better view, a Q^2-increasing constant value (on the right side of the proton panel) has been added to the data which are presented with open and close symbols alternatively. Only data with statistical error lower than 10 μb are shown. The solid curves are the results of Model II calculated for the average Q^2-values in each Q^2-bin. The dashed curves are the predictions of Model II for Q^2=0.

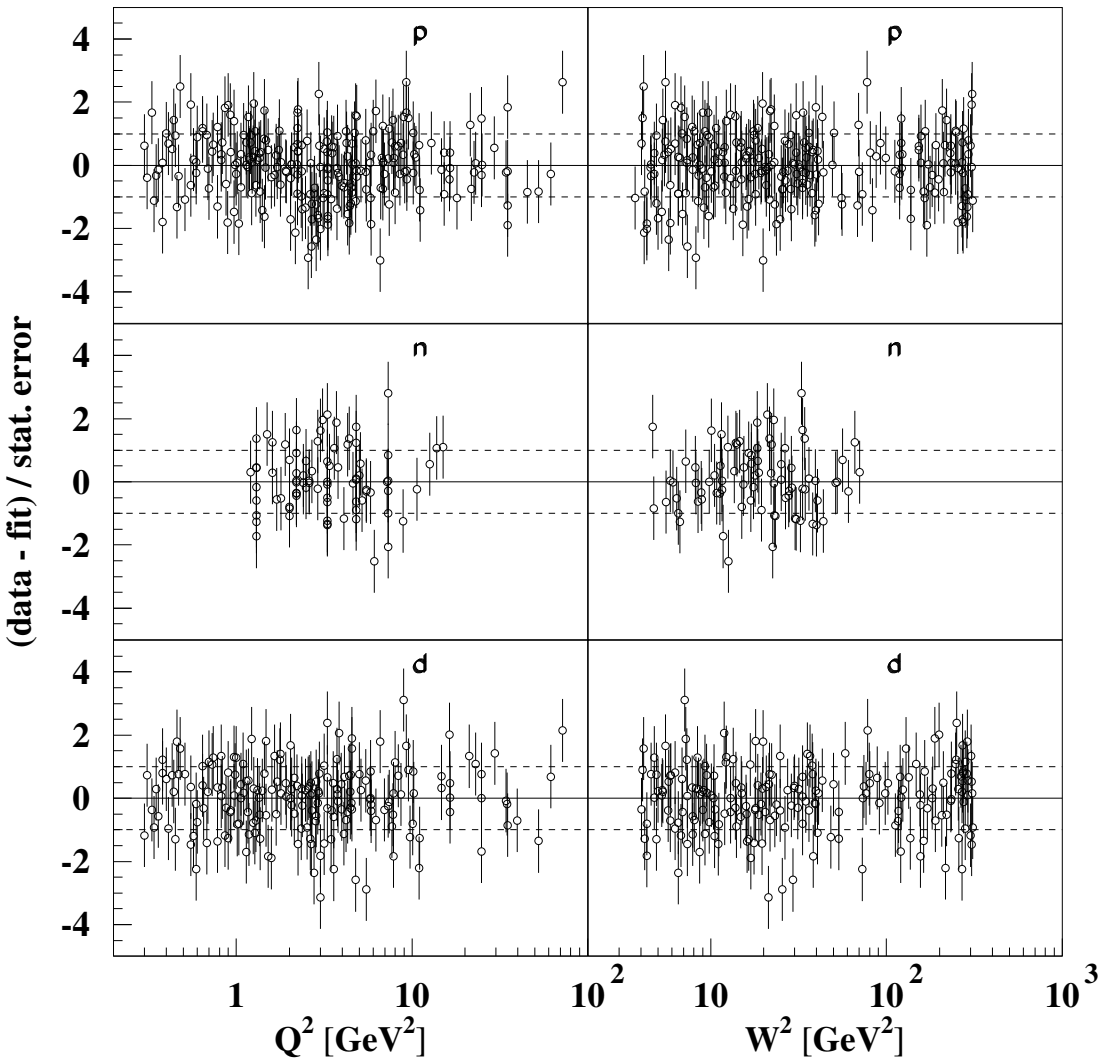

Figure 2: Deviation of the experimental data from the curves of Model II, normalised by the experimental statistical error, as function of Q^2 and of W^2 for the proton, neutron and deuteron.

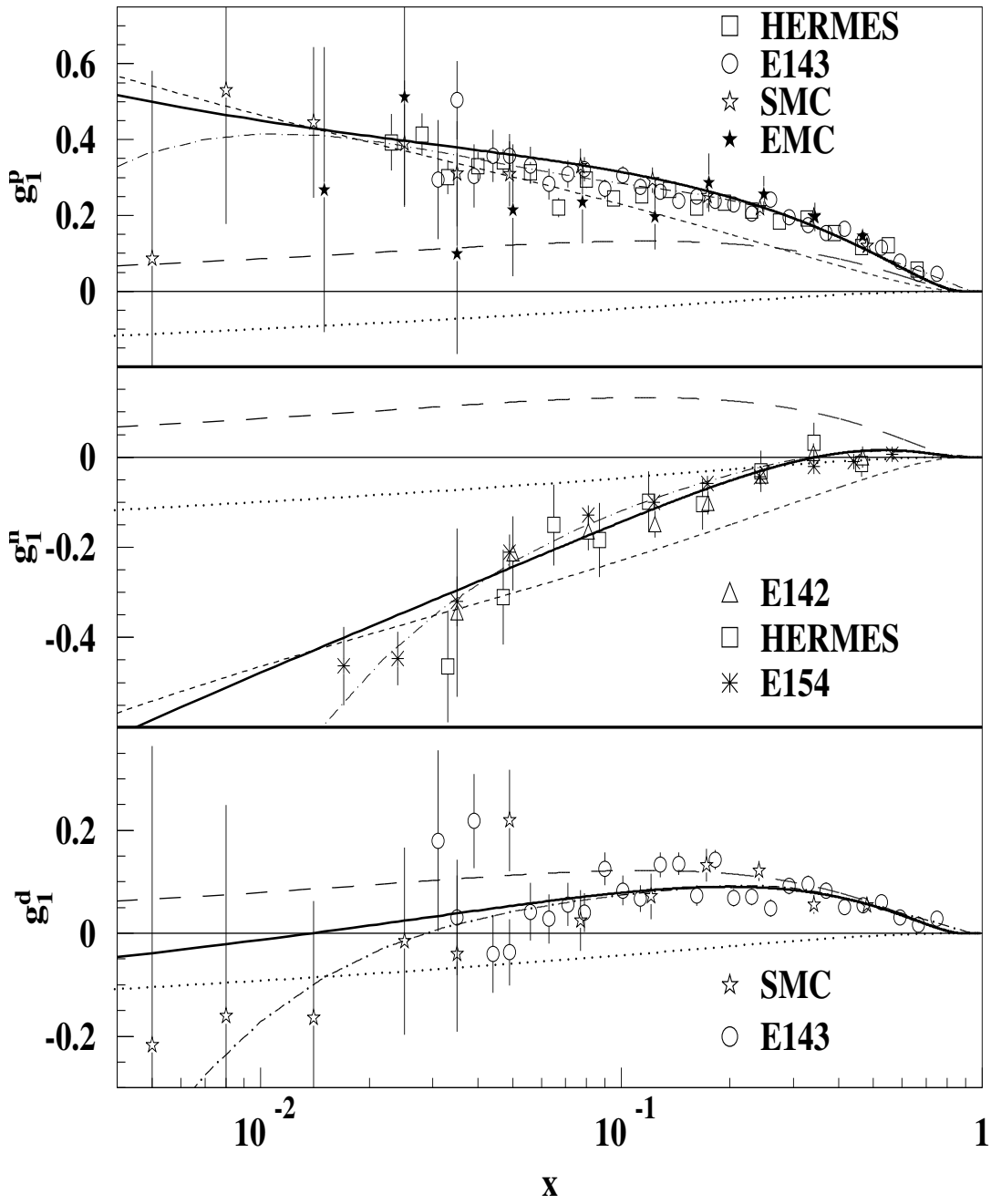

Figure 3: Spin structure functions $g_1(x)$ at $Q^2 = 3$ GeV^2 (same notation as Fig. 1, for the data). The solid curves are the results of Model II. The short-dashed, long-dashed and dotted curves are the a_1, f_1 and two-gluons contributions respectively. The predictions of a NLO-QCD fit [29] are indicated by the dot-dashed curves.

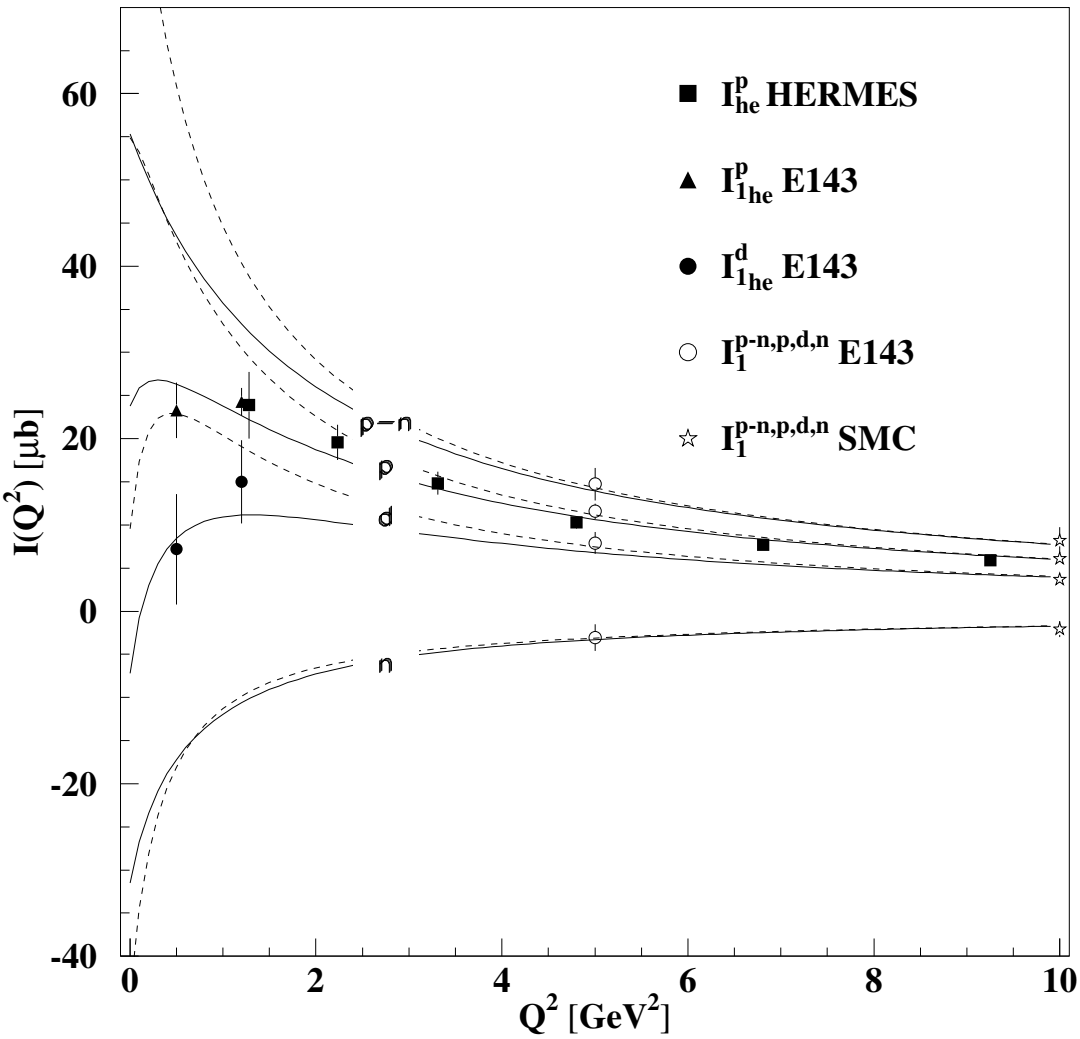

Figure 4: Q^2-evolution of $I_{he}(Q^2)$ (solid curves) and of $I(Q^2)$ (dashed curves) evaluated with Model II for (p-n), p, d and n. The Model predictions are compared with experimental results. The error bars show the quadratic combination of the statistical and the systematic uncertainties.